

ARTICLE **OPEN**


Olfactory marker protein regulation of glucagon secretion in hyperglycemia

 Ju Hun Oh¹, Ye Eon Han¹, Ya Ru Bao¹, Chan Woo Kang¹, JaeHyung Koo¹, Cheol Ryong Ku¹, Yoon Hee Cho³ and Eun Jig Lee^{1,3}

© The Author(s) 2022

The olfactory marker protein (OMP), which is also expressed in nonolfactory tissues, plays a role in regulating the kinetics and termination of olfactory transduction. Thus, we hypothesized that OMP may play a similar role in modulating the secretion of hormones involved in Ca^{2+} and cAMP signaling, such as glucagon. In the present study, we confirmed nonolfactory α -cell-specific OMP expression in human and mouse pancreatic islets as well as in the murine α -cell line $\alpha\text{TC1.9}$. Glucagon and OMP expression increased under hyperglycemic conditions. *Omp* knockdown in hyperglycemic $\alpha\text{TC1.9}$ cells using small-interfering RNA (siRNA) reduced the responses to glucagon release and the related signaling pathways compared with the si-negative control. The $\text{OMP}^{\text{lox}/\text{lox}};\text{GCG}^{\text{cre}/\text{w}}$ mice expressed basal glucagon levels similar to those in the wild-type $\text{OMP}^{\text{lox}/\text{lox}}$ mice but showed resistance against streptozotocin-induced hyperglycemia. The ectopic olfactory signaling events in pancreatic α -cells suggest that olfactory receptor pathways could be therapeutic targets for reducing excessive glucagon levels.

Experimental & Molecular Medicine (2022) 54:1502–1510; <https://doi.org/10.1038/s12276-022-00843-8>

INTRODUCTION

Diabetes mellitus is a chronic metabolic disorder characterized by hyperglycemia. Glucose release into and removal from the circulatory system are important for maintaining normal plasma glucose levels. Insulin is important for controlling plasma glucose levels after meals, as it promotes glucose uptake by peripheral tissues¹. Glucagon secreted from pancreatic α -cells sustains plasma glucose levels in hypoglycemia by stimulating hepatic glucose production². In type 2 diabetes mellitus (T2DM), insulin resistance and defective insulin release are often accompanied by increased glucagon levels, which further mobilize glucose from the liver^{3,4}. Fasting hyperglucagonemia and uncontrolled glucagon levels after meals increase hepatic glucose production and further aggravate diabetes-associated complications. To regulate glucagon secretion, pancreatic α -cells respond appropriately to changes in blood glucose levels (BGLs) by cooperating with both intrinsic and paracrine signals^{5,6}. Although a defective glucagon secretory response causes various problems in patients with diabetes, the mechanisms involved in pancreatic α -cell physiology remain elusive, unlike those in β cell physiology, which have been widely studied.

The olfactory marker protein (OMP) is a 19-kDa cytoplasmic protein that is expressed primarily in mature chemosensory neurons in the main olfactory epithelium^{7,8}. Recently, OMP has been shown to be expressed in nonolfactory tissues, including those in the endocrine system^{9–15}. Previous studies have indicated that OMP acting upstream of cAMP production may be responsible for lowering the elevated Ca^{2+} levels that follow olfactory transduction^{16–18}. In pancreatic α -cells, Ca^{2+} and cAMP are key players in the regulation of glucagon secretion¹⁹. Under physiological conditions, glucagon plays an important role in the

counterregulation of glucose, as it is secreted in response to hypoglycemia²⁰. Under hypoglycemic conditions, elevated cAMP production promotes glucagon release by increasing intracellular Ca^{2+} influx through the plasma membrane, resulting in secretory granules containing glucagon^{21,22}. However, glucagon secretion is inhibited when the glucose concentration is 4–6 mmol/L, which is below the threshold for insulin secretion^{23,24}. In contrast, as the glucose concentration increases above 20 mmol/L, causing maximum stimulation of insulin secretion, glucagon secretion is stimulated, resulting in a U-shaped dose–response^{2,25}. As OMP contributes to regulating the kinetics and termination of olfactory transduction, we hypothesized that it may play a similar role in modulating the secretion of hormones involved in Ca^{2+} and cAMP signaling.

In this study, we investigated the role of OMP, both in vitro and in vivo, in α -cell models and examined the mechanisms underlying the modulation of glucagon secretion to provide a broader understanding of α -cell physiology. Through immunofluorescence staining of human and rodent pancreases, we confirmed that OMP was selectively expressed in α -cells in pancreatic islets.

The results suggest that OMP contributes to regulating the kinetics of intracellular cAMP production in pancreatic α -cells, which changes the secreted glucagon levels. OMP expression in nonolfactory tissues indicates the existence of potential olfactory receptor (OR)-associated events in nonolfactory systems. Thus, future studies on the regulation of glucagon secretion by targeting ORs expressed on α -cells using odorants will be required for the development of novel treatments for diabetes. This study may provide a rationale for novel treatment regimens for diabetes by targeting OMP or OR signaling to modulate glucagon secretion.

¹Brain Korea 21 Project for Medical Science, Yonsei University, College of Medicine, Seoul, South Korea. ²Department of New Biology, DGIST, Daegu 42988, South Korea. ³Division of Endocrinology, Department of Internal Medicine, Yonsei University College of Medicine, Seoul, South Korea. ✉email: wooriminji@gmail.com; ejlee423@yuhs.ac

Received: 16 February 2022 Revised: 30 May 2022 Accepted: 23 June 2022

Published online: 14 September 2022

MATERIALS AND METHODS

Ethical statement

All animal studies were reviewed and approved by the Institutional Animal Care and Use Committee (IACUC) at Yonsei University Health System (approval number: 2015–0025).

Human pancreatic tissue samples

The study was approved by the Institutional Review Board at Yonsei University, and written informed consent was obtained from all subjects (IRB number: 4–2013–0299). Pancreatic tissue was obtained from patients with diabetes and nondiabetic patients undergoing pancreatectomy.

Animal study

Male *OMP*^{−/−} mice were originally developed by Jackson Laboratory (Bar Harbor, ME, USA) and provided by Prof. Jae Hyung Koo, Department of New Biology, DGIST (Daegu, South Korea). Embryos of the *OMP*^{lox/lox}; *GCG*^{cre/w} mice were provided by Prof. Pedro Luis Herrera (University of Geneva, Switzerland). All experimental animals were obtained through embryo transfer at our institution and maintained under controlled conditions (12-h light/dark cycle in a temperature- and humidity-controlled environment) with ad libitum access to food and water. For the experiment, 10-week-old mice were starved for 16 h, and 75 mg/kg STZ (Sigma-Aldrich, St. Louis, MO, USA) was intraperitoneally injected daily for 3 consecutive days in the STZ and experimental groups. STZ powder was freshly diluted in 0.1 M sodium citrate buffer (pH 4.5) immediately before injection. The control group was injected with 0.1 M sodium citrate buffer. Body weight and BGL were measured daily before STZ injection and every 2–4 days after the three consecutive STZ injections. Thirteen days after the first STZ injection, the mice were fasted for 16 h, and an oral glucose tolerance test (OGTT) was performed. BGL was measured at 0, 15, 30, 60, and 120 min after the administration of 2 g/kg glucose by the tail nick bleeding method using a glucometer (Arkray, Minneapolis, MN, USA). Blood samples for hormone analysis were collected using the retro-orbital bleeding method, and serum was isolated by centrifuging the blood at 3000 × *g* for 15 min at 4 °C. After OGTT and blood sample collection, the mice were euthanized by CO₂ inhalation, and pancreatic and liver tissue samples were collected for further analysis. The pancreas of each mouse was fixed in 10% formalin, and paraffin tissue blocks were prepared for staining. The liver tissues were stored in RNAlater solution (Thermo Fisher Scientific, Waltham, MA, USA) at −70 °C until analysis, and RNA and proteins were extracted for the assessment of hepatic enzymes.

Cell culture

For cell culture, we used a glucagon-secreting mouse α TC1 clone 9 (α TC1.9) cell line donated by Prof. Jae Hyung Koo, Department of New Biology, DGIST (Daegu, South Korea). Cells were cultured in Dulbecco's modified Eagle's medium (#31600–034; Thermo Fisher Scientific, Waltham, MA, USA) with 10% (v/v) heat-inactivated FBS, 1% (v/v) penicillin/streptomycin, 2.0 g/L glucose (11.1 mM), 1.5 g/L sodium bicarbonate (17.9 mM), 15 mM HEPES, 0.1 mM nonessential amino acids, and 0.02% (w/v) BSA at 37 °C in a humidified 5% CO₂ incubator.

Plasmid constructs and transfection

siRNA targeting mouse *Omp* (5'-AGC AGC UGG CGU GUC AUG AGG UUG G-3') was purchased from Thermo Fisher Scientific. Before transfection, α TC1.9 cells were seeded at a density of 0.8×10^6 cells/well in 6-well plates for 24 h. siRNA targeting *Omp* or scramble controls (Bioneer, Daejeon, South Korea) was transfected using the Lipofectamine RNAiMAX reagent (Thermo Fisher Scientific) in Opti-MEM medium (Thermo Fisher Scientific) for 16 h. The medium was replaced with culture medium the following day, and the cells were incubated for an additional 24 h before analysis.

Western blotting

Protein lysates were prepared according to the protein extraction protocol (Cell Signaling Technology, Beverly, MA, USA) with 1 mM phenylmethylsulfonyl fluoride and 1× protease inhibitors (Sigma-Aldrich) and quantified using a bicinchoninic acid protein assay kit (Thermo Fisher Scientific). Thereafter, 30–50 μ g of protein lysate was separated by electrophoresis on a 10% SDS-polyacrylamide gel and transferred to polyvinylidene fluoride membranes, which were then blocked with 5% nonfat skim milk and probed with the following primary antibodies at the indicated dilutions: cAMP-responsive element-binding protein (CREB), 1:1000 (#9197); p-CREB,

1:1000 (#9198, all from Cell Signaling Technology, Danvers, MA, USA); and β -actin conjugated horseradish peroxidase (HRP), 1:10000 (47778; Santa Cruz, Paso Robles, CA, USA). The secondary antibody used was donkey anti-rabbit immunoglobulin-horseradish peroxidase antibody (1:5000; Santa Cruz). After incubation with the primary and secondary antibodies, the blots were visualized using a western blotting substrate (WESTSAVEup, AbFrontier, Seoul, South Korea) and exposed to X-ray film (Agfa Healthcare, Mortsel, Belgium). Proteins of interest were quantified using ImageJ v1.51.

Enzyme-linked immunosorbent assay (ELISA)

α TC1.9 cells were seeded in 6-well plates for 24 h before the experiments. On the day of the experiments, the cells were preincubated in Krebs Ringer bicarbonate (KRB) buffer with 10 mM glucose for 30 min and then incubated with different concentrations of glucose in KRB buffer for 15 min. At the time of harvesting the cells, the media were collected and stored at −70 °C until analysis. The secreted glucagon level was assessed using a glucagon DuoSet ELISA kit (DY1249; R&D Systems, Minneapolis, MN, USA), whereas the circulating insulin levels were measured using an ultrasensitive mouse insulin ELISA kit (90080, Crystal Chem, Elk Grove Village, IL, USA) according to the manufacturers' instructions.

RNA isolation, RT-PCR, and quantitative real-time PCR (qRT-PCR)

Total RNA was isolated using NucleoZOL reagent (Macherey-Nagel, Duren, Germany), and cDNA was prepared using ReverTra Ace (TOYOBO, Osaka, Japan) according to the manufacturer's instructions. The resulting cDNA was subjected to either conventional PCR analysis using Ready-2x-Go [Taq] (Nano Helix, Daejeon, South Korea) or quantitative real-time PCR using the Power SYBR Green PCR Master Mix (Applied Biosystems, Foster City, CA, USA) according to the manufacturers' instructions.

Information on the primers used in this experiment is reported in Supplementary Table 1.

Intracellular cAMP measurement

Before the experiments, α TC1.9 cells were seeded in 6-well plates for 24 h. On the day after seeding, the cells were preincubated in KRB buffer with 10 mM glucose. After 30 min, the cells were incubated with a high glucose concentration (30 mM) in KRB buffer for 15 min. The cells were then lysed in 1× cell lysis buffer (Cell Signaling Technology, Beverly, MA, USA) containing 1 mM phenylmethylsulfonyl fluoride dissolved in isopropanol. The protein concentration of 80 μ g was determined using the Bradford assay kit (Bio-Rad Laboratories, Hercules, CA, USA), and equal amounts of proteins were loaded. Intracellular cAMP production was assessed using a cyclic AMP assay kit (#4339, Cell Signaling Technology, Beverly, MA, USA) according to the manufacturer's instructions.

Cell proliferation assay

Before transfection, α TC1.9 cells were seeded at 0.8×10^6 cells/well in 6-well plates for 24 h. Thereafter, siRNA targeting *Omp* or scramble controls (Bioneer, Daejeon, South, Korea) were transfected using the Lipofectamine RNAiMAX reagent (Thermo Fisher Scientific) in Opti-MEM media (Thermo Fisher Scientific) for 16 h. For the 3-(4,5-dimethylthiazol-2-yl)-5-(3-carboxymethoxyphenyl)-2-(4-sulfophenyl)-2H-etrazolium (MTS) assay, the transfected α TC1.9 cells were replated in 96-well plates (5×10^3 cells/well), and cell survival was assessed at 24, 48, and 72 h after transfection. MTS reagent (Promega, Madison, WI, USA) was diluted in culture medium (10 μ L of MTS reagent/100 μ L of culture medium), and the cells were incubated at 37 °C for 1 h. Absorbance at 490 nm was recorded using a plate reader (Thermo Fisher Scientific, Waltham, MA, USA).

Immunofluorescence

Paraffin-embedded samples of the mouse pancreas were cut into 4- μ m-thick sections, deparaffinized in xylene, and rehydrated in a graded series of ethanol. After antigen retrieval in 10 mM sodium citrate buffer (pH 6.0), the sections were blocked with 5% normal donkey serum for 1 h and incubated with anti-OMP (1:100, sc-67219; Santa Cruz, CA, USA), anti-glucagon (1:200, ab10988; Abcam, Cambridge, Waltham, MA, USA), and anti-insulin (1:200, ab181547; Abcam) antibodies overnight at 4 °C. After the sections were washed with Tris-buffered saline containing Tween 20, they were incubated with fluorescence-conjugated secondary antibodies, donkey anti-rabbit-FITC (fluorescein isothiocyanate), donkey anti-goat Cy3, or donkey anti-mouse Cy3 (1:200; Jackson ImmunoResearch, West Grove,

PA, USA) for 2 h at 20–25 °C. After the sections were washed with PBS containing 0.2% Tween, they were mounted in Vectashield mounting medium with DAPI (Vector Laboratories, Burlingame, CA, USA) and visualized using an LSM 700 laser scanning confocal microscope (Carl Zeiss, Oberkochen, Germany). For colocalization of cells expressing FITC-OMP and Cy3-hormone, ImageJ software was used to calculate Pearson's coefficient based on the correlation between red and green signal overlap in at least three different pancreatic tissue sections.

α TC1.9 cells were briefly washed with cold PBS, fixed with 4% paraformaldehyde, and then permeabilized with 1% Triton X-100 in PBS. The cells were blocked with 5% normal donkey serum and then incubated with the primary antibodies overnight at 4 °C. Thereafter, the cells were incubated with the secondary antibodies, mounted in Vectashield mounting medium with DAPI, and visualized using an LSM 700 laser scanning confocal microscope (Carl Zeiss).

Mouse pancreatic islet isolation

Pancreatic islets of 13- to 15-week-old male mice were isolated. Mice were sacrificed with CO₂ inhalation, and an incision was made immediately around the upper abdomen to expose the liver and intestines. After the ampulla was clamped, 2 mL of liberase solution (1.9 mL RPMI-1640 media + 0.1 mL liberase) was injected into the pancreas through the common bile duct using a 30-gauge needle. The pancreas was carefully removed from the intestine, placed in a 50 mL conical tube containing 2 mL of liberase solution (Roche Holding AG, Basel, Switzerland) and digested for 15 min at 37 °C in a water bath. The conical tube was shaken every 5 min to ensure that the pancreas was completely digested. After complete digestion, 10 mL of Hanks' balanced salt solution with 0.3% BSA and 1% penicillin/streptomycin was added and filtered through a sieve with a pore size of 200 μ m. The islets collected into new conical tubes were centrifuged at 330 \times g for 2 min, and the supernatant was removed. Islets were resuspended in 10 mL of cold 1100 Histopaque (Sigma-Aldrich, St. Louis, MO, USA), and 10 mL of Hanks' balanced salt solution was carefully added to the top and then centrifuged at 900 \times g for 18 min. Isolated islets were poured onto a 100- μ m cell strainer, and captured islets were collected into 10-cm culture dishes in RPMI-1640 media with 10% FBS and 1% penicillin/streptomycin. After overnight incubation, islets were hand-picked using a pipette for experiments. Forty islets per sample were used for ELISAs, 150–200 islets per sample were used for western blot analysis, and each experiment was performed in the same way as the α TC1.9 cell line.

Statistical analysis

Statistical analyses were carried out using GraphPad Prism software v.4.0.0 (GraphPad, Inc., La Jolla, CA, USA). Each experiment was performed at least three times. Statistical significance was determined using one-way ANOVA, followed by post hoc Tukey analysis and Student's *t*-test to compare the means of two different groups. $p < 0.05$ was considered to indicate significance. Differences are indicated using asterisks (* $p < 0.05$; ** $p < 0.01$; *** $p < 0.001$). All measurements were taken from distinct samples.

RESULTS

OMP is involved in glucagon secretion by pancreatic α -cells

In a previous study, we demonstrated that OMP is expressed only in mouse pancreatic α -cells among the three main types of hormone-producing pancreatic cells²⁶. Therefore, we hypothesized that ectopic *Omp*-mediated events would occur in pancreatic α -cells. First, we compared the expression patterns of OMP in human pancreatic islets of nondiabetic individuals and patients with diabetes (Fig. 1a). Consistent with our previous findings, the colocalization of OMP and glucagon was verified in the α -cells of human pancreatic islets.

In the current study, the number of OMP-positive cells was found to be higher in the pancreatic tissues of the patients with diabetes than in those of the nondiabetic individuals. We further examined OMP expression in the glucagon-secreting murine α -cell line α TC1.9 and confirmed the suitability of the cell line for studying the functional role of OMP in α -cells.

In α TC1.9 cells, the colocalization of OMP and glucagon was confirmed, and when the glucose concentration increased from 5

to 30 mM, the expression of OMP and glucagon increased (Fig. 1b). In α TC1.9 cells, glucagon secretion was reduced when the glucose concentration increased from 0 to 5 mM. Conversely, we noted a significant increase in glucagon secretion when the glucose concentration reached 30 mM ($p < 0.001$). Consistent with the findings of previous studies^{20,23,27}, we observed a U-shaped dose–response for glucose-regulated glucagon secretion in α TC1.9 cells (Fig. 1c). Interestingly, the *Omp* mRNA levels showed a pattern similar to that of glucose-regulated glucagon secretion ($p < 0.01$ at 30 mM) (Fig. 1d). The changes in intracellular cAMP and p-CREB levels were also consistent with the established pattern of glucagon secretion in response to different glucose concentrations (Fig. 1e, f).

Glucagon secretion in isolated pancreatic islets of *Omp*^{+/+} and *Omp*^{-/-} mice

To investigate the role of OMP in glucagon secretion independent of systemic effects, we isolated pancreatic islets of wild-type *Omp*^{+/+} and *Omp*^{-/-} mice. No significant differences were observed between the wild-type *Omp*^{+/+} and *Omp*^{-/-} islets in morphology or size (Fig. 2a). In the wild-type *Omp*^{+/+} islets, the response to different glucose concentrations also showed U-shaped curves similar to those of α TC1.9 cells. However, in the *Omp*^{-/-} islets, the response to both low and high glucose concentrations was blunted. Secretion under 5 mM basal glucose conditions was slightly but not significantly higher than that of the wild-type *Omp*^{-/-} islets (Fig. 2b). This result was in agreement with our in vitro and in vivo experiments. In the *Omp*^{-/-} islets, AMPK phosphorylation was reduced (Fig. 2c). Inhibition of AMPK phosphorylation at 30 mM glucose was not as dramatic in the *Omp*^{-/-} islets as the wild-type *Omp*^{+/+} islets (Fig. 2c). Additionally, phosphorylation of CREB at 5 mM glucose was increased in the *Omp*^{-/-} islets, which is comparable to the 30 mM glucose condition of the *Omp*^{+/+} islets. However, at 30 mM glucose, phosphorylation of CREB was attenuated in the *Omp*^{-/-} islets. These findings suggest that isolated pancreatic islets respond to different glucose concentrations in a dose-dependent U-shaped manner, as in α TC1.9 cells.

Effect of *Omp* knockdown on glucose-dependent glucagon secretion in α TC1.9 cells

To determine whether the modulation of OMP expression would affect glucagon secretion and related pathways, we treated α TC1.9 cells with siRNA directed against *Omp* (siOMP) and found that the *Omp* mRNA levels were significantly reduced (* $p < 0.05$). Under hyperglycemic conditions, the increase in *Omp* expression was significantly higher in the negative control (siNEG) cells than in the OMP knockdown α -cells (### $p < 0.01$) (Fig. 3a). Consistent with these results, the mRNA levels of *Gcg* were increased in the negative control group (* $p < 0.05$) when the glucose concentration was 30 mM (Fig. 3b). In contrast, 30 mM glucose decreased glucagon expression (## $p < 0.01$ vs. siNEG, Fig. 3c) and CREB phosphorylation (Fig. 3h) in the siOMP-transfected α TC1.9 cells. In the *Omp* knockout animal models, olfactory response kinetics and termination are slowed by 2- to 8-fold due to modulation in cAMP kinetics¹⁷. Therefore, we investigated whether elevated glucagon secretion is due to altered cAMP kinetics in the siOMP-transfected group of α TC1.9 cells (Fig. 3d–g). For control samples, a rise in cAMP levels occurs at early time points and gradually decreases at 5 mM glucose concentrations, and there is a peak at 15 min at 30 mM glucose. In the siOMP-transfected samples, the kinetics seemed to be delayed, as cAMP levels at 5 min were higher than those at 1 min for 5 mM glucose concentrations, and the peak concentration for the 30 mM glucose concentration was at 30 min. Interestingly, the overall secretions in the siOMP-transfected α TC1.9 cells were elevated compared with those in the control, although stimulation of these cells was attenuated at the high glucose concentration. These results indicate that there is a delay

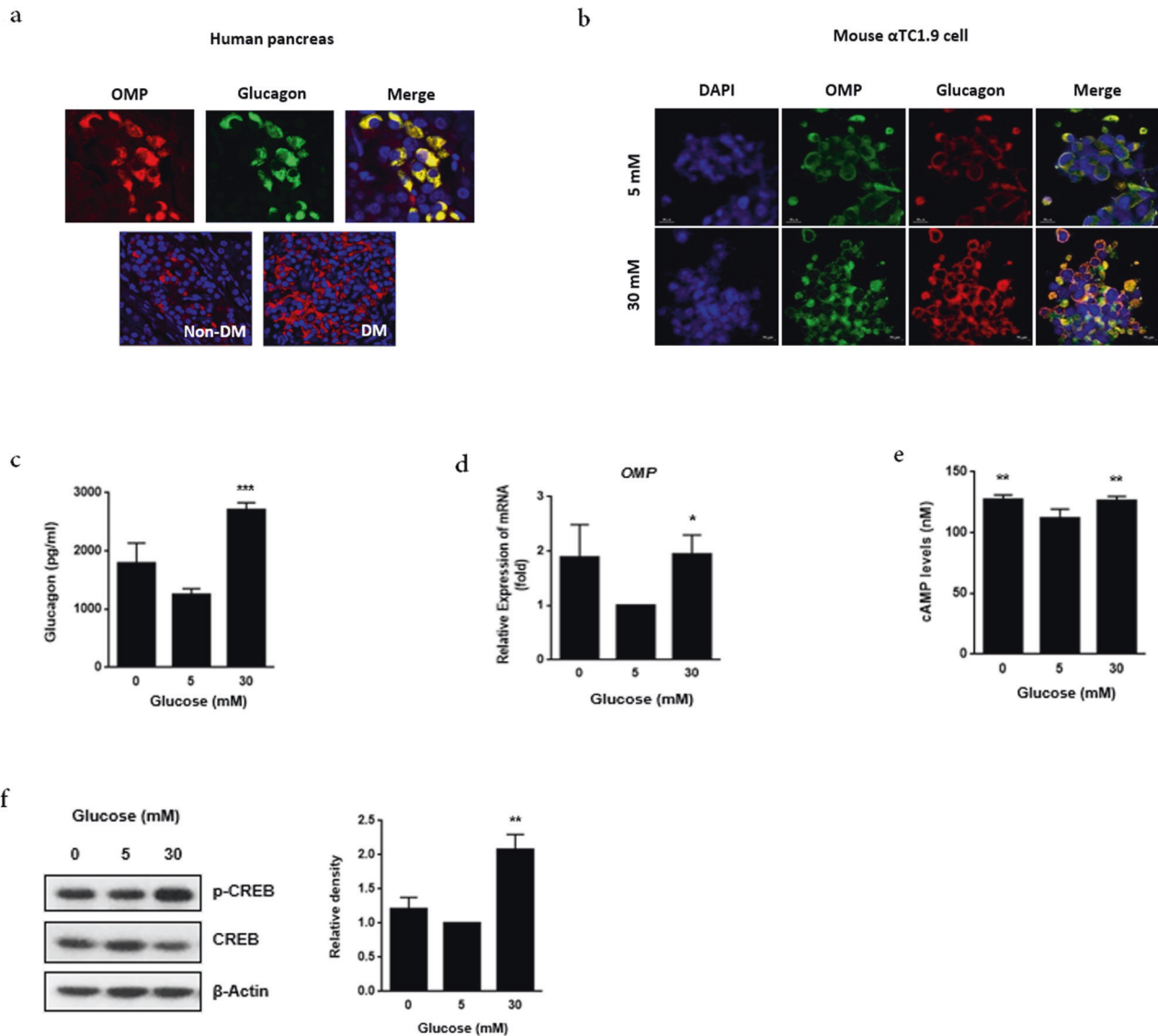


Fig. 1 Olfactory marker protein (OMP) is involved in glucose dose-response U-shaped glucagon secretion by pancreatic α -cells. Immunofluorescence staining demonstrated the colocalization of **a** OMP (red) and glucagon (green) in the human pancreas and **b** OMP (green) and glucagon (red) in mouse pancreatic α TC1.9 cells. Images were obtained using a laser scanning microscope at 200x magnification. qRT-PCR analysis of **c** proglucagon (*Gcg*) expression and **d** *Omp* expression in α TC1.9 cells. The mRNA level of each gene was normalized to that of *Gapdh*. Each value is presented as the mean \pm SD of three independent experiments. * $p < 0.05$, ** $p < 0.01$ vs. siNEG, 5 mM glucose, # $p < 0.05$, ## $p < 0.01$ vs. siNEG, 30 mM glucose. **e** Intracellular cAMP levels were analyzed with the indicated glucose concentration for 15 min in α TC1.9 cells. **f** CREB phosphorylation was analyzed using western blotting after 15 min of incubation of cells with the indicated glucose concentrations. Bands are representative of three independent experiments. The two-tailed Student's *t*-test was used to determine statistical significance. Error bars indicate the standard deviations. * $p < 0.05$, ** $p < 0.01$, *** $p < 0.001$ vs. 5 mM glucose.

in cAMP responses to glucose when *Omp* is knocked down, which results in elevated glucagon secretion. Cell survival was assessed using the MTS assay to investigate whether glucagon secretion and related pathways were enhanced due to increased cell proliferation. However, we found that *Omp* knockdown had no impact on cell survival (Fig. 3i).

Glucose homeostasis is altered following STZ induction in the $OMP^{lox/lox};GCG^{cre/w}$ mice

Next, we examined whether OMP plays a physiological role in glucagon secretion and glucose homeostasis using the $OMP^{lox/lox};GCG^{cre/w}$ transgenic mouse model. The control (sodium citrate) groups of both wild-type $OMP^{lox/lox}$ mice and $OMP^{lox/lox};GCG^{cre/w}$ mice showed a similar weight range, and weight loss following STZ injection decreased similarly in both the

wild-type $OMP^{lox/lox}$ STZ ($p < 0.005$ vs. the wild-type $OMP^{lox/lox}$ control on Day 11) and the $OMP^{lox/lox};GCG^{cre/w}$ STZ groups ($p < 0.001$ vs. the wild-type $OMP^{lox/lox}$ control on Day 11) (Fig. 4a). The feeding BGL of the STZ-injected wild-type $OMP^{lox/lox}$ mice reached 593.7 ± 31.0 mg/dL, whereas that of the $OMP^{lox/lox};GCG^{cre/w}$ mice reached 446.3 ± 40.5 mg/dL on Day 11 (## $p < 0.01$, ### $p < 0.005$ vs. wild-type $OMP^{lox/lox}$ STZ) (Fig. 4b).

OGTT revealed no glycemic excursions in the $OMP^{lox/lox};GCG^{cre/w}$ and wild-type $OMP^{lox/lox}$ mice and that the former was significantly resistant to STZ-induced hyperglycemia (# $p < 0.05$ at 30 and 60 min) (Fig. 4c). We hypothesized that the significant resistance against STZ-induced hyperglycemia in the $OMP^{lox/lox};GCG^{cre/w}$ mice was caused by altered glucagon secretion from OMP-deleted α -cells. As expected, the responses of the $OMP^{lox/lox};GCG^{cre/w}$ mice to oral glucose administration were different from those of the wild-

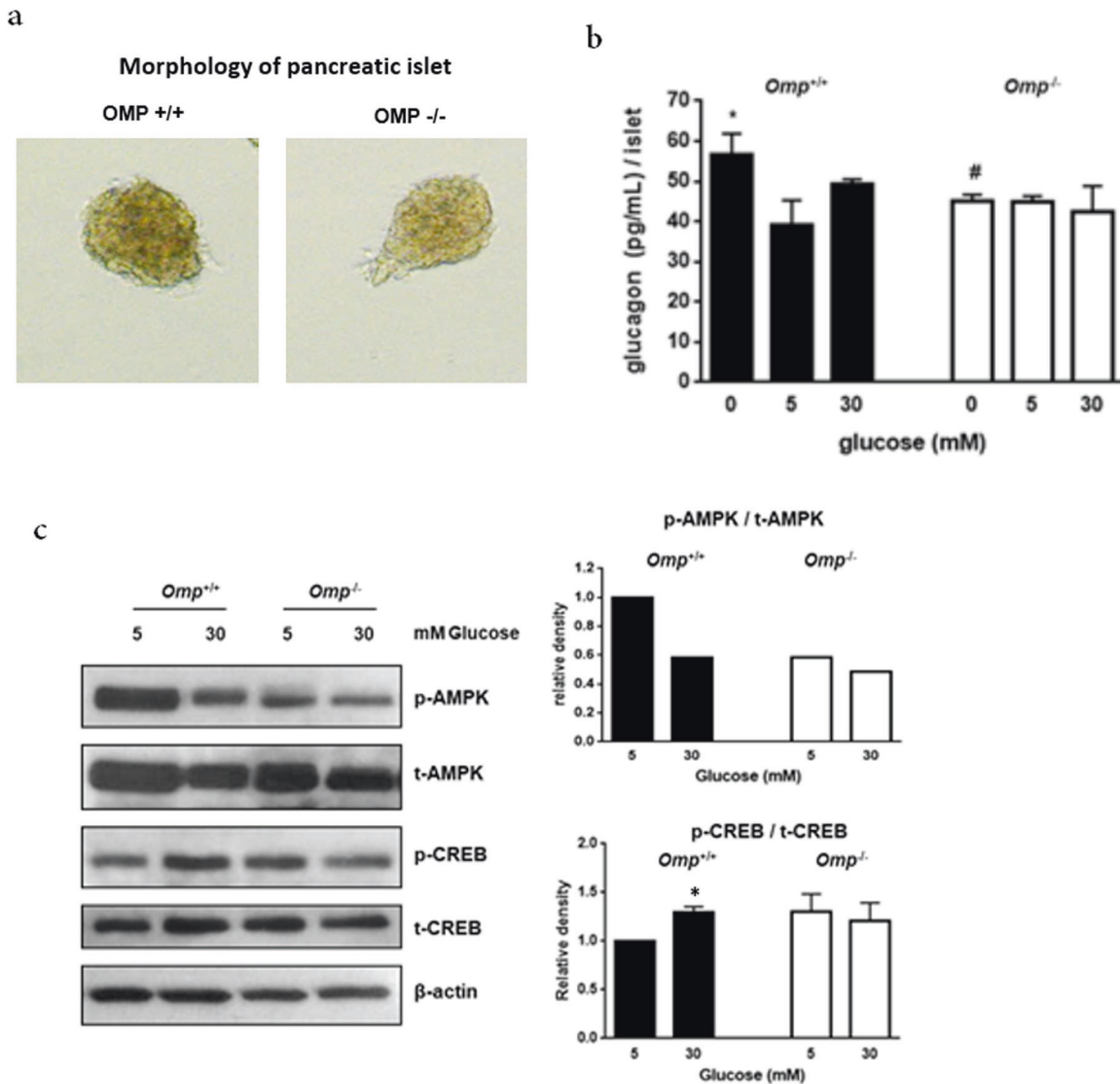


Fig. 2 Olfactory marker protein (OMP) is required for glucagon secretion stimulated by high glucose concentrations in isolated mouse pancreatic islets. **a** Morphology of isolated pancreatic islets of the $Omp^{+/+}$ and $Omp^{-/-}$ mice at 10 weeks. **b** Secreted glucagon levels of isolated pancreatic islets of the $Omp^{+/+}$ ($n=4$) and $Omp^{-/-}$ ($n=6$) mice treated with different concentrations of glucose for 45 min. **c** Phosphorylation of CREB and AMPK was analyzed using western blot analysis after 45 min of incubation with glucose at the indicated concentrations. Phosphorylation of AMPK and CREB was quantified by densitometry and normalized to total AMPK and CREB, respectively, for each sample. The two-tailed Student's *t*-test was used to determine statistical significance. Error bars indicate the standard deviations. * $p < 0.05$, ** $p < 0.01$, *** $p < 0.001$ vs. 5 mM glucose, # $p < 0.05$, ## $p < 0.01$ vs. $Omp^{+/+}$ at each glucose concentration.

type $Omp^{lox/lox}$ mice. In the fasting state, the basal glucagon levels in the $Omp^{lox/lox};GCG^{cre/w}$ and $Omp^{lox/lox}$ control mice were similar. However, STZ-induced fasting glucagon secretion levels were significantly lower (## $p < 0.01$) in the $Omp^{lox/lox};GCG^{cre/w}$ mice (480.6 ± 31.1 pg/mL) than in the control mice (703.8 ± 76.1 pg/mL) (Fig. 4d). Moreover, STZ injection reduced insulin secretion in both the control and $Omp^{lox/lox};GCG^{cre/w}$ mice (Fig. 4e). As shown in Fig. 4d, the expression of glucagon in pancreatic islets showed a pattern similar to that of glucagon secretion. The expression of glucagon was increased in pancreatic islets of the STZ-treated wild-type $Omp^{lox/lox}$ mice, whereas it was decreased in the $Omp^{lox/lox};GCG^{cre/w}$ mice (Fig. 4f). These findings suggest that *Omp* plays a key role in glucagon secretion changes following STZ induction in the $Omp^{lox/lox};GCG^{cre/w}$ mice.

As the liver is the main target organ for glucagon, where it stimulates hepatic glucose production^{28–30}, the expression levels of hepatic enzymes were assessed. As expected, the mRNA levels of enzymes involved in gluconeogenesis, including

glucose 6-phosphatase (*G6Pase*) ($p < 0.05$) and phosphoenolpyruvate carboxykinase (*Pepck*), were upregulated in the STZ-stimulated $Omp^{+/+}$ mice and $Omp^{lox/lox}$ mice, while STZ-induced glucagon secretion was blunted in the $Omp^{-/-};Omp^{lox/lox};GCG^{cre/w}$ mice, so *Pepck* and *G6pase* expression was reduced ($p < 0.01$) (Fig. 4g).

DISCUSSION

OMP is selectively expressed in the main olfactory epithelium and has also been shown to play roles in nonolfactory tissues, including endocrine tissues^{7,8,26,31}. In the olfactory system, the binding of specific ligands to ORs expressed on the surface of OR neurons initiates a signal transduction cascade involving G_{olf} , adenylyl cyclase (type III), and OMP, which leads to increased intracellular cAMP production and Ca^{2+} influx. Accumulating evidence indicates that OMP might be important in Ca^{2+} extrusion, acting upstream of cAMP production^{17,18,32}.

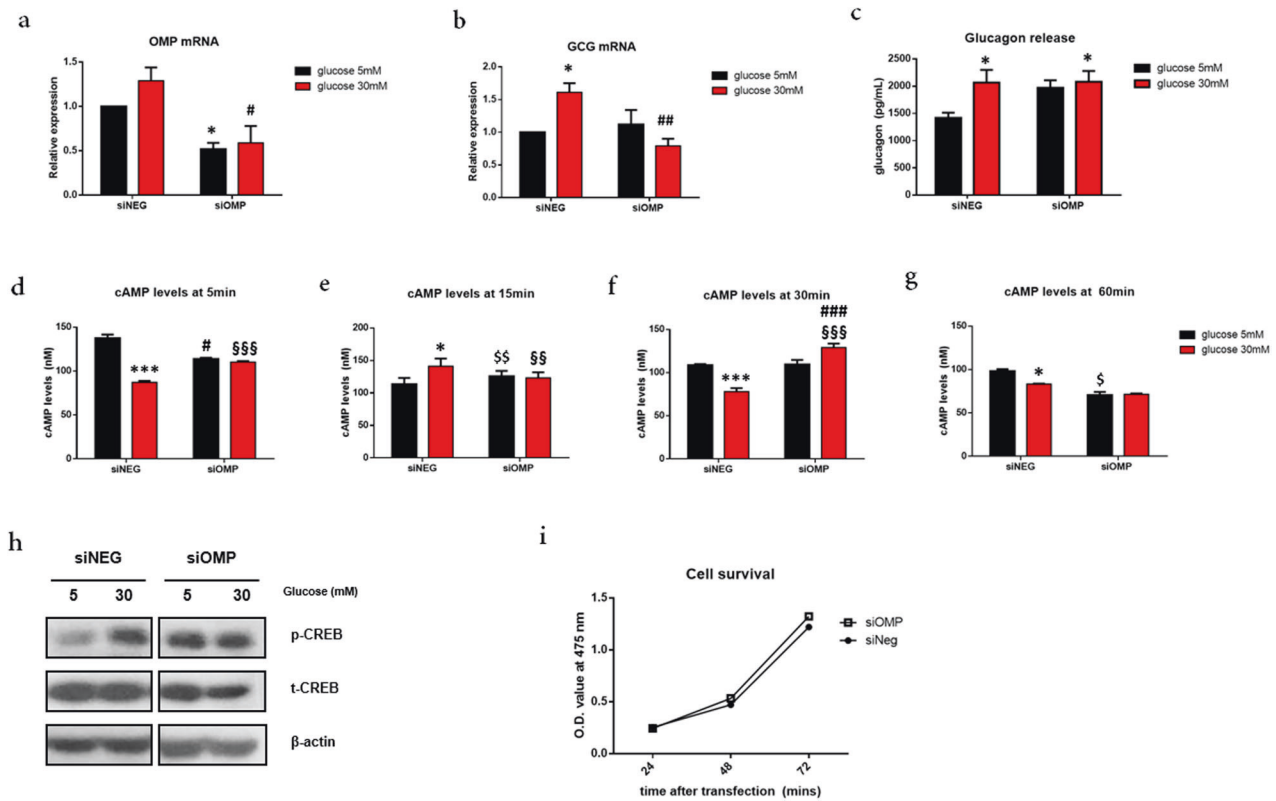


Fig. 3 Olfactory marker protein (OMP) knockdown alters the cAMP response, resulting in decreased glucagon secretion at high glucose concentrations. **a**, **b** qRT-PCR analysis of **a** *Omp* expression and **b** proglucagon (*Gcg*) expression after transfection with *Omp*-specific siRNA in α TC1.9 cells. **c** Analysis of secreted glucagon levels in conditioned medium of transfected α TC1.9 cells with different concentrations of glucose. **d–g** Intracellular cAMP levels were analyzed with the indicated glucose concentration for 15 min in α TC1.9 cells transfected with siNEG or siOMP. * $p < 0.05$, siNEG 5 mM glucose vs. siNEG 30 mM glucose, # $p < 0.05$, siOMP 5 mM glucose vs. siOMP 30 mM glucose, \$ $p < 0.05$, siNEG 5 mM glucose vs. siOMP 5 mM glucose, \$\$ $p < 0.05$, siNEG 30 mM glucose vs. siOMP 30 mM glucose. **h** CREB phosphorylation was analyzed using western blotting after 15 min of incubation of transfected cells with the indicated glucose concentrations. **i** After transfection, α TC1.9 cell survival was assessed using the MTS assay at the indicated time points. The two-tailed Student's *t*-test was used to determine statistical significance. Error bars indicate the standard deviations. * $p < 0.05$, vs. 5 mM glucose, # $p < 0.05$, ## $p < 0.01$ vs. siScramble at each glucose concentration.

In pancreatic α -cells, Ca^{2+} and cAMP are key messengers in the regulation of glucagon secretion³³. Under hypoglycemic conditions, increased cAMP production promotes glucagon release by increasing Ca^{2+} influx, resulting in the exocytotic release of secretory granules containing glucagon^{21,22}. Under normal physiological conditions, glucose inhibits glucagon secretion by lowering the Ca^{2+} concentration in a cell. However, when the glucose concentration exceeds a specific threshold, above 25 mmol/l, glucose stimulates the release of glucagon independent of the Ca^{2+} concentration. Instead, glucagon secretion is further promoted by cAMP²⁷. As OMP plays a role in regulating the kinetics and termination of olfactory transduction involving Ca^{2+} and cAMP signaling, we hypothesized that OMP may play a similar role in modulating glucagon secretion in pancreatic α -cells.

In a previous study, immunofluorescence staining for OMP and the three main pancreatic hormones, glucagon, somatostatin, and insulin, to determine the expression of OMP in pancreatic islets of mice revealed that OMP is specifically expressed in glucagon-positive α -cells; immunofluorescence staining of the human pancreas showed similar results²⁶. After confirming the expression of OMP in the glucagon-secreting murine α -cell line α TC1.9, we investigated whether the modulation of OMP expression would affect glucose-regulated glucagon secretion and related signaling pathways. Interestingly, *Omp* knockdown in α TC1.9 cells increased basal glucagon secretion as well as intracellular cAMP levels and CREB phosphorylation.

In the olfactory system, the absence of OMP results in delayed time-to-transient-peak of response, latency to first spike, and response termination. These phenomena have been demonstrated to be caused by the increased overall basal activity due to the prolonged response of cAMP in *Omp*^{-/-} mice in response to odors¹⁷. Recent studies have reported that OMP directly binds cAMP to regulate the level of freely available cAMP and to control the basal cAMP pool^{34–36}. Thus, by buffering the cAMP levels, OMP prevents persistent depolarization of OR neurons, enabling a sustained response to repeated stimuli. We predicted that, like α -cells, OMP would bind newly generated cAMP to prevent excessive surge and enable glucagon secretion. As expected, delayed intracellular cAMP kinetics were observed when *Omp* was knocked down, resulting in elevated overall basal glucagon secretion. Interestingly, in the siOMP-transfected α -cells, stimulation by low or high glucose concentrations was attenuated. Increased basal activity and prolonged response of cAMP in the absence of OMP indicate that OMP works upstream of cAMP production. Moreover, *Omp* knockdown resulted in weak cAMP buffering and reduced glucagon secretion due to sustained depolarization after the initial cAMP surge. OMP knockdown does not affect cell proliferation; therefore, glucagon secretion changes are independent of α -cell proliferation.

As in the in vitro experiments, circulating glucagon levels in the control groups were not significantly different between the wild-type *OMP*^{lox/lox} and *OMP*^{lox/lox};GCG^{cre/w} mice under fasting basal conditions. However, the increase in glucagon release due to STZ-

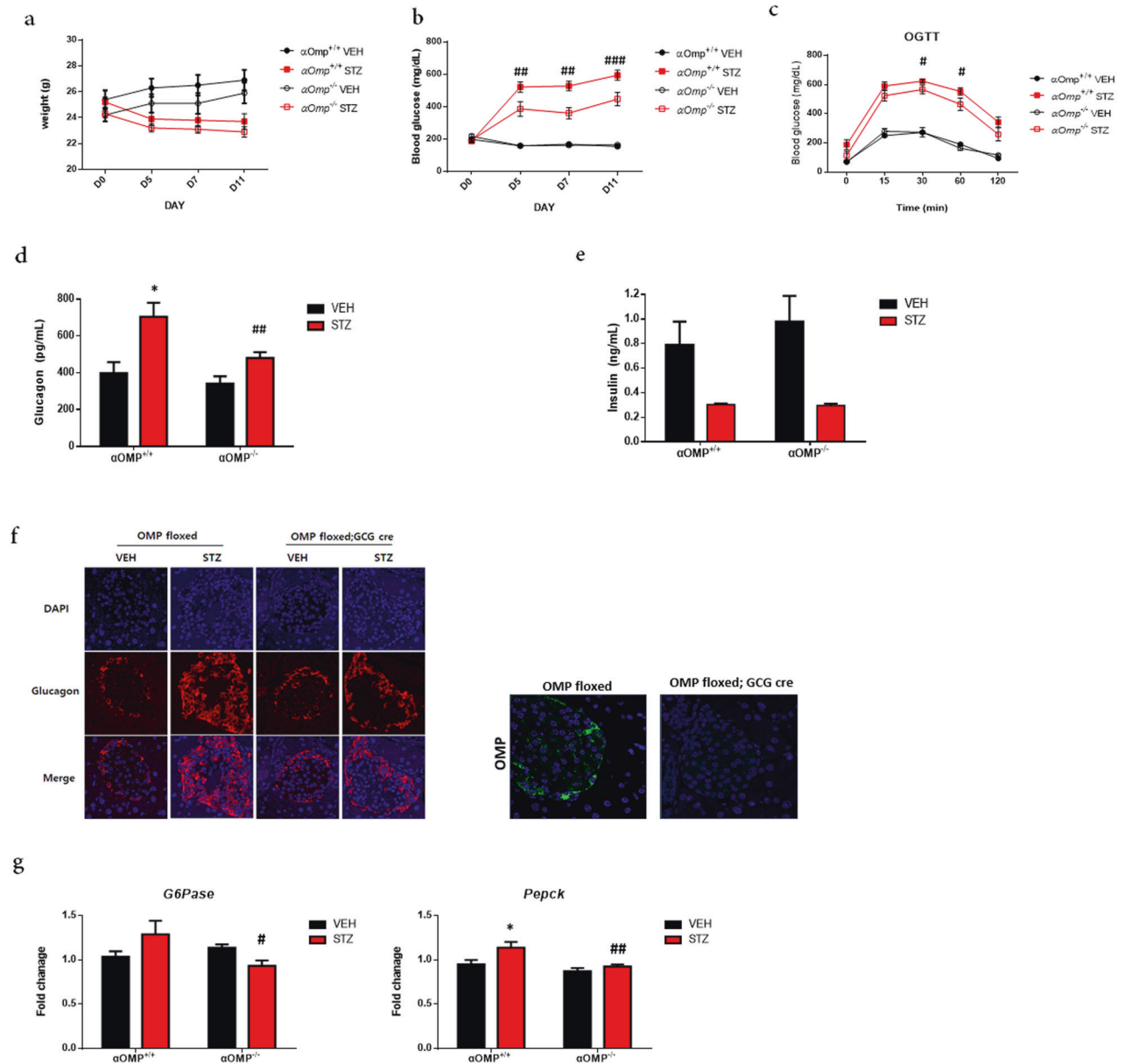


Fig. 4 Olfactory marker protein (OMP) is required for high glucose concentration-induced glucagon secretion in α cells of mice. **a** Body weight changes in the $\text{OMP}^{\text{lox/lox}}$ ($\alpha\text{Omp}^{+/+}$) mice and $\text{OMP}^{\text{lox/lox};\text{GCG}^{\text{cre/w}}}$ ($\alpha\text{Omp}^{-/-}$) mice before and after STZ injection. **b** Blood glucose level changes. $\#\#p < 0.01$, $\#\#\#p < 0.001$ vs. $\text{OMP}^{\text{lox/lox}}$ STZ. **c** OGTT was performed on Day 13 after STZ injection. On Day 13 after STZ induction, fasting basal glucagon (**d**) and insulin (**e**) levels were measured. **f** Expression of glucagon (red) and OMP (green) in the pancreatic islets of the $\text{OMP}^{\text{lox/lox};\text{GCG}^{\text{cre/w}}}$ mice with STZ-induced hyperglycemia. The two-tailed Student's *t*-test was used to determine statistical significance. Error bars indicate the standard deviations. $*p < 0.05$ vs. VEH, in each group, $\#p < 0.05$, $\#\#p < 0.01$, $\#\#\#p < 0.001$ vs. $\alpha\text{Omp}^{+/+}$ STZ. **g** At Day 13 after STZ induction, mice were sacrificed, and liver enzymes were analyzed. The expression of *G6pase* and *Pepck* was analyzed using qRT-PCR analysis in $\alpha\text{Omp}^{+/+}$ and $\alpha\text{Omp}^{-/-}$. The two-tailed Student's *t*-test was used to determine statistical significance. Error bars indicate the standard deviations. $*p < 0.05$ vs. VEH, in each group, $\#p < 0.05$, $\#\#p < 0.01$ vs. $\alpha\text{Omp}^{+/+}$ STZ.

induced hyperglycemia was significantly lower in the $\text{OMP}^{\text{lox/lox};\text{GCG}^{\text{cre/w}}}$ mice than in the wild-type $\text{OMP}^{\text{lox/lox}}$ mice. Consistent with this result, OGTT demonstrated that the $\text{OMP}^{\text{lox/lox};\text{GCG}^{\text{cre/w}}}$ mice had significantly fewer glycemic excursions than the wild-type $\text{Omp}^{+/+}$ mice. As there were no significant changes in the plasma levels of insulin and GLP-1, which are important hormones controlling BGL, the altered glucose homeostasis in the $\text{OMP}^{\text{lox/lox};\text{GCG}^{\text{cre/w}}}$ mice may arise due to changes in glucagon secretion.

Moreover, the expression of enzymes in the liver, which is the main target organ of glucagon, was affected by altered glucagon release³⁰. Under normal physiological conditions, glucagon

stimulates the export of glucose from the liver by increasing the rates of glycogenolysis and gluconeogenesis and suppressing glycolysis^{37,38}. As the basal circulating glucagon levels decreased in the $\text{OMP}^{\text{lox/lox};\text{GCG}^{\text{cre/w}}}$ mice, the mRNA levels of enzymes involved in gluconeogenesis, including *G-6pase* ($p < 0.01$) and *Pepck*, were decreased in STZ-induced hyperglycemia. Consequently, the STZ-injected $\text{OMP}^{\text{lox/lox};\text{GCG}^{\text{cre/w}}}$ mice were more resistant to hyperglycemia than the $\text{OMP}^{\text{lox/lox}}$ mice.

Nevertheless, there are certain limitations to this study. We did not determine whether the changes in glucagon secretion due to OMP are limited to STZ-induced hyperglycemia alone or diabetes in general, such as high-fat diet-induced hyperglycemia. However,

we used STZ-injected mice because we excluded factors that regulate glucagon secretion except for OMP. STZ damages pancreatic β -cells, which secrete insulin, thus inhibiting glucagon secretion and inducing hyperglycemia. Therefore, the STZ-induced diabetic mouse model was more suitable to study the relationship between OMP and glucagon secretion.

In conclusion, OMP is responsible for regulating the cAMP kinetics of glucagon secretion in α -cells of the pancreatic islet. In vitro studies using α TC1.9 cells revealed that delayed responses in cAMP kinetics to different glucose concentrations result in elevated glucagon secretion when OMP is absent. The basal secretion of glucagon was already elevated; therefore, stimulatory effects at low and high glucose concentrations were attenuated. Notably, the fasting circulating glucagon levels in the OMP^{lox/lox};GCG^{cre/w} mice were similar to those in the wild-type OMP^{lox/lox} mice, but the degree of hyperglucagonemia induced by STZ was significantly reduced in the former, resulting in significant resistance against STZ-induced hyperglycemia.

Our findings provide evidence that OMP expression in α -cells has a physiological role in regulating glucagon secretion, especially in hyperglycemia. The finding of ectopic olfactory signaling events in pancreatic α -cells suggests that OR pathways could be targets for reducing glucagon levels in patients with diabetes. Inhibiting olfactory signaling in diabetic α -cells could allow the development of novel treatment regimens for diabetes.

REFERENCES

- Alberti, K. G. & Zimmet, P. Z. Definition, diagnosis and classification of diabetes mellitus and its complications. Part 1: diagnosis and classification of diabetes mellitus provisional report of a WHO consultation. *Diabet. Med.* **15**, 539–553 (1998).
- D'Alessio, D. The role of dysregulated glucagon secretion in type 2 diabetes. *Diabetes Obes. Metab.* **13**, 126–132 (2011).
- Jiang, G. & Zhang, B. B. Glucagon and regulation of glucose metabolism. *Am. J. Physiol. Endocrinol. Metab.* **284**, E671–E678 (2003).
- Edgerton, D. S. & Cherrington, A. D. Glucagon as a critical factor in the pathology of diabetes. *Diabetes* **60**, 377–380 (2011).
- Olofsson, C. S., Salehi, A., Göpel, S. O., Holm, C. & Rorsman, P. Palmitate stimulation of glucagon secretion in mouse pancreatic α -cells results from activation of L-type calcium channels and elevation of cytoplasmic calcium. *Diabetes* **53**, 2836–2843 (2004).
- Zhang, Q. et al. Role of KATP channels in glucose-regulated glucagon secretion and impaired counterregulation in type 2 diabetes. *Cell Metab.* **18**, 871–882 (2013).
- Buiakova, O. I. et al. Olfactory marker protein (OMP) gene deletion causes altered physiological activity of olfactory sensory neurons. *Proc. Natl Acad. Sci. USA* **93**, 9858–9863 (1996).
- Youngentob, S. L., Margolis, F. L. & Youngentob, L. M. OMP gene deletion results in an alteration in odorant quality perception. *Behav. Neurosci.* **115**, 626–631 (2001).
- Kang, N. et al. Olfactory marker protein expression is an indicator of olfactory receptor-associated events in non-olfactory tissues. *PLoS ONE* **10**, e0116097 (2015).
- Ferrer, I. et al. Olfactory receptors in non-chemosensory organs: the nervous system in health and disease. *Front. Aging Neurosci.* **8**, 163 (2016).
- Chang, A. J., Ortega, F. E., Riegler, J., Madison, D. V. & Krasnow, M. A. Oxygen regulation of breathing through an olfactory receptor activated by lactate. *Nature* **527**, 240–244 (2015).
- Pluznick, J. L. et al. Olfactory receptor responding to gut microbiota-derived signals plays a role in renin secretion and blood pressure regulation. *Proc. Natl Acad. Sci. USA* **110**, 4410–4415 (2013).
- Kang, C. W. et al. Olfactory marker protein regulates prolactin secretion and production by modulating Ca²⁺ and TRH signaling in lactotrophs. *Exp. Mol. Med.* **50**, 15 (2018).
- Han, Y. E. et al. Olfactory receptor OR51E1 mediates GLP-1 secretion in human and rodent enteroendocrine L cells. *J. Endocr. Soc.* **2**, 1251–1258 (2018).
- Wu, C. et al. Olfactory receptor 544 reduces adiposity by steering fuel preference toward fats. *J. Clin. Invest.* **127**, 4118–4123 (2017).
- Dibattista, M. & Reisert, J. The odorant receptor-dependent role of olfactory marker protein in olfactory. *J. Neurosci.* **36**, 2995–3006 (2016).
- Reisert, J., Yau, K. W. & Margolis, F. L. Olfactory marker protein modulates the cAMP kinetics of the odour-induced response in cilia of mouse olfactory receptor neurons. *J. Physiol. (Lond.)* **585**, 731–740 (2007).
- Matthews, H. R. & Reisert, J. Calcium, the two-faced messenger of olfactory transduction and adaptation. *Curr. Opin. Neurobiol.* **13**, 469–475 (2003).
- Tian, G., Sandler, S., Gylfe, E. & Tengholm, A. Glucose- and hormone-induced cAMP oscillations in α - and β -cells within intact pancreatic islets. *Diabetes* **60**, 1535–1543 (2011).
- Cryer, P. E., Davis, S. N. & Shamoon, H. Hypoglycemia in diabetes. *Diabetes Care* **26**, 1902–1912 (2003).
- Johansson, H., Gylfe, E. & Hellman, B. Cyclic AMP raises cytoplasmic calcium in pancreatic α 2-cells by mobilizing calcium incorporated in response to glucose. *Cell Calcium* **10**, 205–211 (1989).
- Ma, X. et al. Glucagon stimulates exocytosis in mouse and rat pancreatic α -cells by binding to glucagon receptors. *Mol. Endocrinol.* **19**, 198–212 (2005).
- Olsen, H. L. et al. Glucose stimulates glucagon release in single rat α -cells by mechanisms that mirror the stimulus-secretion coupling in β -cells. *Endocrinology* **146**, 4861–4870 (2005).
- Vieira, E., Salehi, A. & Gylfe, E. Glucose inhibits glucagon secretion by a direct effect on mouse pancreatic α cells. *Diabetologia* **50**, 370–379 (2007).
- Quesada, I., Tuduri, E., Ripoll, C. & Nadal, A. Physiology of the pancreatic α -cell and glucagon secretion: role in glucose homeostasis and diabetes. *J. Endocrinol.* **199**, 5–19 (2008).
- Kang, N. et al. Olfactory receptor Olfr544 responding to azelaic acid regulates glucagon secretion in α -cells of mouse pancreatic islets. *Biochem. Biophys. Res. Commun.* **460**, 616–621 (2015).
- Salehi, A., Vieira, E. & Gylfe, E. Paradoxical stimulation of glucagon secretion by high glucose concentrations. *Diabetes* **55**, 2318–2323 (2006).
- Ramnanan, C. J., Edgerton, D. S., Kraft, G. & Cherrington, A. D. Physiologic action of glucagon on liver glucose metabolism. *Diabetes Obes. Metab.* **13**, 118–125 (2011).
- Lin, H. V. & Accili, D. Hormonal regulation of hepatic glucose production in health and disease. *Cell Metab.* **14**, 9–19 (2011).
- Kawamori, D. et al. Insulin signaling in α cells modulates glucagon secretion in vivo. *Cell Metab.* **9**, 350–361 (2009).
- Kang, N. & Koo, J. Olfactory receptors in non-chemosensory tissues. *BMB Rep.* **45**, 612–622 (2012).
- Dibattista, M. & Reisert, J. The odorant receptor-dependent role of olfactory marker protein in olfactory receptor neurons. *J. Neurosci.* **36**, 2995–3006 (2016).
- Tian, G., Sandler, S., Gylfe, E. & Tengholm, A. Glucose- and hormone-induced cAMP oscillations in α - and β -cells within intact pancreatic islets. *Diabetes* **60**, 1535–1543 (2011).
- Nakashima, N. et al. Olfactory marker protein directly buffers cAMP to avoid depolarization-induced silencing of olfactory receptor neurons. *Nat. Commun.* **11**, 2188 (2020).
- Nakashima, N., Nakashima, K., Nakashima, A. & Takano, M. Olfactory marker protein captures cAMP produced via Gas-protein-coupled receptor activation. *Biochem. Biophys. Res. Commun.* **529**, 341–346 (2020).
- Nakashima, N., Nakashima, K., Nakashima, A. & Takano, M. Olfactory marker protein elevates basal cAMP concentration. *Biochem. Biophys. Res. Commun.* **531**, 203–208 (2020).
- Ramnanan, C., Edgerton, D., Kraft, G. & Cherrington, A. Physiologic action of glucagon on liver glucose metabolism. *Diabetes Obes. Metab.* **13**, 118–125 (2011).
- Miller, R. A. & Birnbaum, M. J. Glucagon: acute actions on hepatic metabolism. *Diabetologia* **59**, 1376–1381 (2016).

ACKNOWLEDGEMENTS

We acknowledge Dr. Pedro Luis Herrera, Geneva University, Switzerland for providing glucagon Cre-mice for our studies. This research was supported by a grant from the Korea Health Technology R&D Project through the Korea Health Industry Development Institute (KHIDI), funded by the Ministry of Health & Welfare, South Korea (grant number: HR18C0012) and by the Basic Science Research Program through the National Research Foundation of Korea (NRF) funded by the Ministry of Education (grant number: 2020R11A1A01074357).

AUTHOR CONTRIBUTIONS

Conceived and designed the experiments: E.J.L., Y.H.C., and C.R.K. Performed the experiments: J.H.O., Y.E.H., Y.R.B., C.W.K., and Y.H.C. Analyzed the data: J.H.O., Y.E.H., and Y.H.C. Contributed reagents/materials/analysis tools: J.H.O., Y.E.H., Y.R.B., C.W.K., C.R.K., and J.H.K. Wrote the paper: J.H.O., Y.E.H., and Y.H.C. J.H.O. and Y.E.H. had full access to all the data in the study and take responsibility for the integrity of the data and the accuracy of the data analysis. The authors declare no competing interests.

COMPETING INTERESTS

The authors declare no competing interests.

ADDITIONAL INFORMATION

Supplementary information The online version contains supplementary material available at <https://doi.org/10.1038/s12276-022-00843-8>.

Correspondence and requests for materials should be addressed to Yoon Hee Cho or Eun Jig Lee.

Reprints and permission information is available at <http://www.nature.com/reprints>

Publisher's note Springer Nature remains neutral with regard to jurisdictional claims in published maps and institutional affiliations.



Open Access This article is licensed under a Creative Commons Attribution 4.0 International License, which permits use, sharing, adaptation, distribution and reproduction in any medium or format, as long as you give appropriate credit to the original author(s) and the source, provide a link to the Creative Commons license, and indicate if changes were made. The images or other third party material in this article are included in the article's Creative Commons license, unless indicated otherwise in a credit line to the material. If material is not included in the article's Creative Commons license and your intended use is not permitted by statutory regulation or exceeds the permitted use, you will need to obtain permission directly from the copyright holder. To view a copy of this license, visit <http://creativecommons.org/licenses/by/4.0/>.

© The Author(s) 2022